Journal of The Electrochemical Society, **149** (6) B265-B271 (2002)
0013-4651/2002/149(6)/B265/7/$7.00 © The Electrochemical Society, Inc.

The Correlation Between Substrate Mass Loss and Electrochemical Impedance Spectroscopy Data for a Polymer-Coated Metal

D. B. Mitton,[a,*,z] S. L. Wallace,[a] N. J. Cantini,[a] F. Bellucci,[b,*] G. E. Thompson,[c,] N. Eliaz,[a,***] and R. M. Latanision[a,*]**

[a]*H. H. Uhlig Corrosion Laboratory, Department of Materials Science and Engineering, Massachusetts Institute of Technology, Cambridge, Massachusetts 02139, USA*
[b]*Department of Materials and Production Engineering, University of Naples Federico II, 80125 Naples, Italy*
[c]*Corrosion and Protection Centre, University of Manchester Institute of Science and Technology, Manchester M60 1QD, United Kingdom*

Research has been carried out to evaluate the correlation between substrate mass loss and data generated by electrochemical impedance spectroscopy (EIS). Experiments were carried out as a function of exposure time for both polymer-coated and bare samples. Mass loss was determined *in situ* and in real time with a vibrating sample magnetometer (VSM). In all cases, the sample was held potentiostatically at the open circuit potential (OCP) while EIS data were collected. Mass loss data calculated from electrochemical impedance (EI) spectra were then compared to equivalent data generated on the VSM. Although previous research has investigated the correlation for bare samples [W. J. Lorenz and F. Mansfeld, *Corros. Sci.*, **21**, 647 (1981)] establishing this relationship for a coated substrate is more convoluted. The difficulty results from errors associated with solution uptake within the polymer, and corrosion product entrapment. Such errors obviate the use of traditional gravimetric techniques and, until now, the relationship between substrate mass loss and EIS has not unequivocally been established for polymer-coated samples. Although the current research indicates that EIS can accurately define the mass loss for a bare sample, the correlation for coated samples has, generally, not been as good.
 [DOI: 10.1149/1.1473777]

Manuscript submitted December 26, 2000; revised manuscript received January 11, 2002. Available electronically April 25, 2002.

One methodology for reducing corrosion damage is painting or coating with an organic, and one of the most widely employed techniques for evaluating such polymer-coated systems is electrochemical impedance spectroscopy (EIS). Although the association between EIS data and mass loss for noncoated metals was previously described,[1] the analogous relationship for polymer-coated metals was not accurately defined prior to the current research. The difficulties in substrate mass loss determination are associated with solution uptake within a polymer, and corrosion product entrapment at the coating/metal interface. Such errors obviate the use of traditional gravimetric techniques. During the current study, the metallic mass loss for a polymer-coated metal was assessed and correlated to equivalent data produced by EIS. This was accomplished by utilizing a vibrating sample magnetometer (VSM) to magnetically quantify the mass loss for a polymer-coated cobalt substrate. These data were then correlated to corresponding mass loss data assessed by EIS.

While degradation depends on a number of variables,[2] coatings isolate the substrate from direct contact with the environment and by retarding the arrival of reactants at the interface. Such coatings, however, tend to contain pores, defects, and virtual pores (Fig. 1), and, ultimately, underfilm corrosion is still likely to develop.

When a material corrodes, it experiences a change in mass as a function of exposure time, and mass loss is, in many respects, the reference measurement against which all other techniques are assessed. During an electrochemical reaction, the proportionality between the current (I) and mass reacted (m) is defined by Faraday's law

$$m = \frac{Ita}{nF} \qquad [1]$$

where m is the change in mass, I is the current, t is time, a is the atomic mass, n is the valence change of the metal in the reaction, and F is Faraday's constant (96,486 C/equivalent). The cumulative mass loss (m_T) at any time (t) is obtained by substituting the Stern-Geary relationship[3] for I and summing the mass change (m) determined for individual exposure periods between the time 0 and t

$$m_T = \sum_0^t \left[\frac{at}{nFR_p} \cdot \frac{\beta_a|\beta_c|}{2.3(\beta_a + |\beta_c|)} \right] \qquad [2]$$

In this relationship β_a and β_c are termed the anodic and cathodic Tafel constants, and R_p is the polarization resistance.

EIS is currently employed to rank coatings, assess interfacial reactions, quantify coating breakdown, and predict the lifetime of coating/metal systems.[4] The most common circuit employed for polymer-coated systems is presented in Fig. 2. In this figure, R_s is the electrolyte resistance, R_f and C_f are the film resistance and capacitance and R_{ct} and C_{dl} represent the charge-transfer resistance and the double-layer capacitance. Diffusional processes are represented by the Warburg impedance (Z_w), which can be related to blockage of oxygen diffusion paths by corrosion products.[5-7] For a nondegraded polymer-coated metal system, before the interface becomes active, only the external circuit (R_s, R_f, C_f) will be observed experimentally. With time, however, the inner circuit (R_{ct}, C_{dl}, Z_w) may also become active, and this is the source of a second time constant. The appearance of the latter has been linked with system breakdown. The two time constants represent the film (τ_f) at higher frequencies and the metal (τ_m) at lower frequencies. In order to determine the rate of corrosion and, hence, the mass loss, the R_p or R_{ct}, value needs to be detected. While in the simplest situation, R_{ct} and R_p may be equivalent, these values are not necessarily the same.[1,8] In addition, one potential problem during EIS analysis is data validity,[9] and the limitations associated with the technique need to be considered.

Magnetic measurements may also be used to monitor corrosion. The curves presented in Fig. 3 reveal the relationship between the magnetizing force (H), and the magnetic flux density (B) for a Co sample assessed on a VSM before and after corrosion. When the applied field exceeds the saturating field for a ferromagnetic material such as Co, the magnetization becomes independent of the applied field and the saturation magnetization, M_s (the maximal mag-

* Electrochemical Society Active Member.
** Electrochemical Society Fellow.
*** Electrochemical Society Student Member.
z E-mail: bmitton@mit.edu

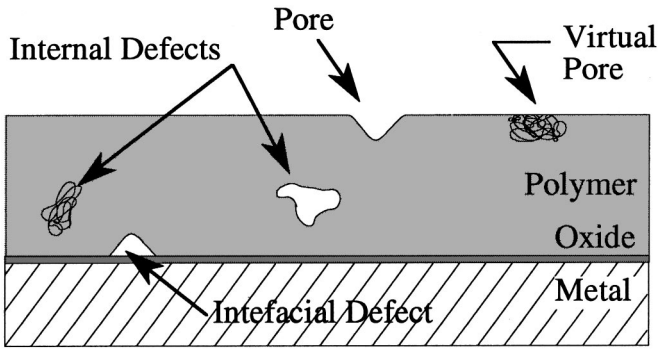

Figure 1. Schematic representation of a polymer-coated metal system.

netic moment density) is reached. As this parameter is directly related to the volume of cobalt, the mass loss can readily be assessed by measuring the difference in the magnetic saturation (ΔM_s).[10,11]

This paper addresses some unresolved issues remaining in spite of significant research in the area of protective organic coatings. During this study, the metallic mass loss for a polymer-coated magnetic metal has been assessed and correlated to data produced by EIS. This work provides insight into the interpretation of impedance spectra for the evaluation and assessment of coating performance.

Experimental

Preliminary experimental work.—The primary goal of this research was to determine mass loss for a polymer-coated system by employing the VSM and to compare this to the mass loss determined by EIS. Prior to performing more advanced research, it was necessary to establish the accuracy of the VSM in determining mass change for the samples used during the current study.

In this section, the mass loss assessed by gravimetric, electrochemical, and magnetic methods is compared. The data not only indicate that the methodology is possible, but they also reveal a 1:1 relationship between mass loss (%) and ΔM_s (%).

Vibrating sample magnetometer.—A model 880 VSM from Digital Measurement Systems, Inc., was employed to determine ΔM_s during this project. This instrument measures the magnetic moment of a sample by vibrating it perpendicular to an applied magnetic field. An induced voltage occurs in the stationary detection coils due to the magnetic field of the sample. Reference coils in the VSM, also experience a voltage induced by a reference sample attached to the drive rod. The vibrating frequency of the reference and test samples are identical, thus the voltages can be related to one another, resulting in an accurate measurement of the magnetic moment of the test sample. Since changes of magnetic moment as small as 10^{-5} emu are theoretically detected,[12] mass loss on the order of few micrograms are possible. The optimal sample placement in space is termed the saddle point, and is critical for accurate measurement[13] as, at this point, the signal is independent of small displacements with respect to the detection coils. While the best sample geometry for the magnetic measurements is an ellipsoid of relatively small size compared to the detection coils,[13,14] the preferred geometry for EIS requires a relatively large exposed area. Larger samples are accommodated either by calibrating with a standard sample of comparable geometry[13] or by applying the appropriate corrections.

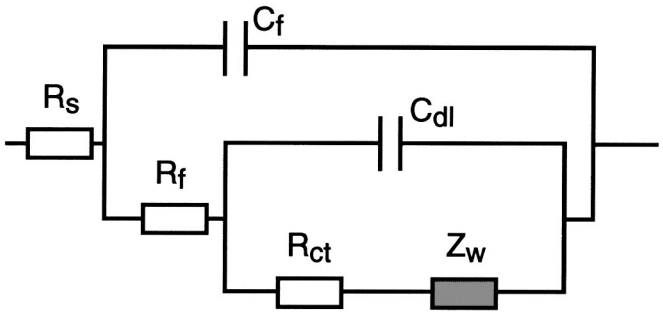

Figure 2. The equivalent circuit frequently used to represent polymer-coated systems. In this figure, R_s is the electrolyte resistance, R_f and C_f are the film resistance and capacitance and R_{ct}, C_{dl}, and Z_w represent the charge-transfer resistance, double-layer capacitance, and Warburg impedance, respectively.

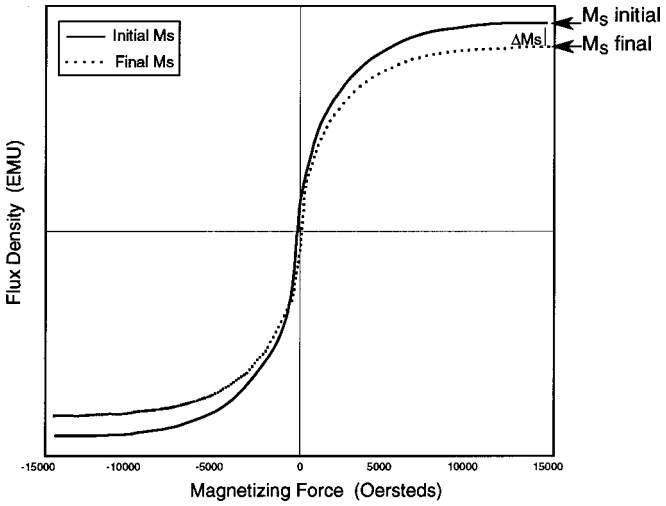

Figure 3. The relationship between the magnetizing force (H) and the magnetic flux density (B) for a Co sample assessed on a VSM before and after corrosion.

Electrochemical cell design.—Fe, Ni, and Co were the practical ferromagnetic substrate metals of choice for this project. Cobalt was selected as the metallic substrate both for the ferromagnetic character of the parent metal and for the nonferromagnetic properties of the corrosion products.[15] In the first case, the loss of metal required to produce an identical change in magnetic saturation is smaller for Co than for Ni, enabling smaller metallic mass loss increments to be detected. In the second case, while cobalt oxides such as CoO and Co_3O_4 are nonferromagnetic,[16] some iron corrosion products (Fe_3O_4, for example) exhibit a significant magnetic character. The latter could result in an erroneous mass loss determination similar to that associated with the incomplete removal of corrosion products at the termination of a traditional mass loss experiment.

During this phase of the work,[11] both Co-coated Si wafers and Co foils were used. For samples produced from foils, a 0.25 mm thick, 99.95% pure Co foil from Alpha Æsar was used. For samples produced from Si wafers, wafers were E-beam deposited (Microsystems Technology Laboratory at MIT) to a thickness of 3200 Å from a 99.95% pure Co target, and the thickness of the layer was inspected both by profilometer (Tencor-KLA P10) and confocal scanning laser microscopy (Lasertec 1LM21).

Samples were coated at the University of Naples with a transparent acrylic varnish mixed from Viacryl VSC 5754/60 and Maprenal MF800 (Vianova Resins). To encourage rapid degradation, varnish viscosity was systematically altered to provide a high coating defect density, and the polymer was intentionally undercured to decrease cross-linking and to increase permeability to moisture and ions.

A three-electrode system incorporating Pt foil as the counter electrode, a saturated calomel electrode (SCE) as reference, and a cobalt sample as the working electrode was used for the electrochemical cell. Connection to the working electrode was provided by an insulated copper wire. The wire attachment area and sample edges were sealed with Amercoat 90 (Ameron). During potentiodynamic and potentiostatic experiments, the reference electrode was

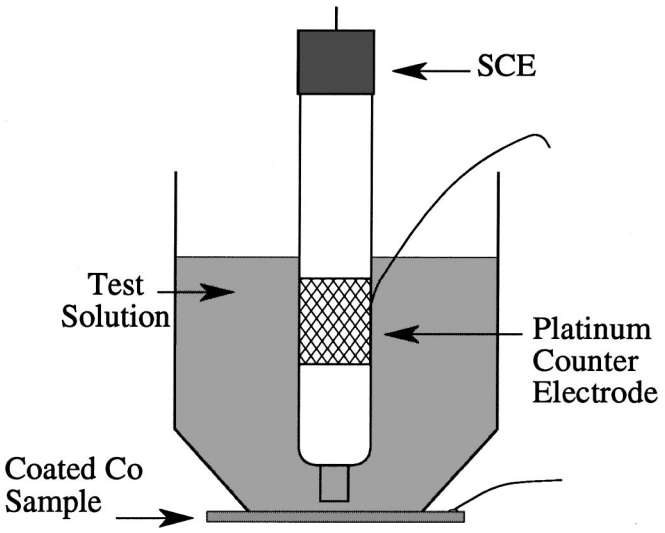

Figure 4. The electrochemical cell used for EIS during the preliminary experimental work.

located in a separate vessel and a solution bridge and Luggin capillary were employed. During EIS experiments, however, the counter electrode was secured to the reference electrode and both were immersed in the test solution (Fig. 4). The electrolyte employed was 0.5 M NaCl. In all cases a Solartron 1260 impedance/gain-phase analyzer was used in combination with either a Schlumberger Solartron 1286 or 1287 electrochemical interface. Experiments were controlled or analyzed by dc Corrware, ZPlot, or Zview (Scribner Associates) or by EISTEST, a software package developed in the H.H. Uhlig Corrosion Laboratory.

Results and Discussion

Potentiodynamic experiments.—Initial potentiodynamic experiments were conducted in order to determine the most appropriate parameters for subsequent potentiostatic tests. Experiments were carried out in a neutral aqueous 0.5 M NaCl electrolyte at ambient temperature. A representative curve for a cobalt-coated Si wafer in 0.5 M NaCl is presented in Fig. 5. The decrease in current in the potential range −240 to −100 mV (SCE) indicates the onset of passivation previously observed for a Co-20Ni alloy.[10] The current decrease at higher potentials, is likely due to the removal of the majority of the cobalt layer. Upon completion of such a scan, the

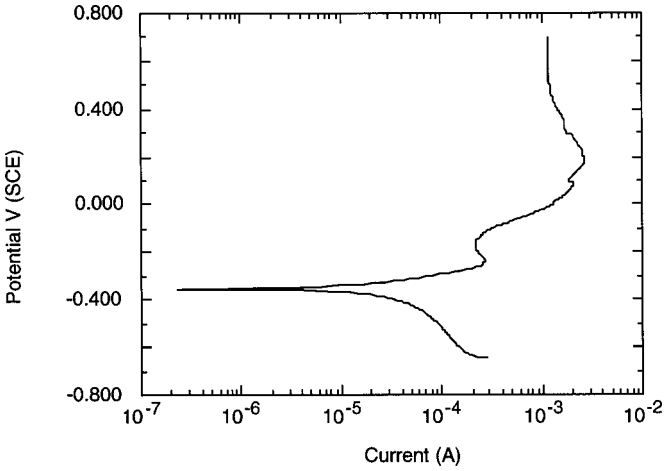

Figure 5. A potentiodynamic curve representative of the bare cobalt-coated Si wafer system used during the current study.

mass loss for the wafer samples was on the order of 60% of the total metal available, and the Si substrate was visible in discrete areas. During potentiodynamic tests, the OCP was in the range −360 to −380 mV *vs.* SCE and Tafel slopes were generally determined to be approximately 0.081 and 0.367 V/decade for the anodic and cathodic regions, respectively.

Correlation of mass loss for the various techniques.—Since it is easier to control the magnitude of mass loss, potentiostatic experiments have been employed to generate the data used to assess the correlation among gravimetric mass loss, VSM data, and electrochemical results. For each individual test, after cleaning, a bare cobalt foil was weighed on a balance (Mettler AE 200) and then characterized on the VSM (average of 7-10 VSM curves generally having a confidence level of at least 95%).

The sample was then held at a potential for a time designed to provide a mass loss in the range 1-11% of the available metal. After an experiment, samples were immediately rinsed with DI water to remove any salt or lightly adhering corrosion product. More tenacious products were removed by cleaning ultrasonically in deionized (DI) water. Samples were subsequently recharacterized on the VSM and reweighed. In addition, data were integrated to determine the area under the current-time curve and, thus, provide the value of the coulombs associated with the corrosion of the sample. The mass loss for the sample was calculated with Eq. 1. Figure 6 presents the correlation between the gravimetricly determined mass loss and the mass loss determined (a) magnetically and (b) electrochemically. The results indicate that the magnetic saturation data and electrochemical mass loss data display a linear 1:1 relationship with the gravimetric mass loss data. In addition, these results indicate an exceptionally good correlation among the three measurement techniques, and the percentage of mass loss based on change in magnetic saturation correlates exactly to the mass loss determined both electrochemically and gravimetrically.

The change in M_s, which can accurately be detected by the VSM, is on the order of 0.5-1.0% of the total M_s of the sample. As a result of this instrument limit, the smallest mass change increment detectable by VSM for the Co foil samples used during this phase of the study was 3 mg. Such a large increment was considered unsatisfactory for assessing underfilm corrosion, where mass losses could be significantly lower. It was possible, however, by employing samples with a lower total M_s (Co-coated Si wafers) to reduce the minimum detectable mass loss increment to approximately 5 μg.

Electrochemical impedance spectroscopy (EIS).—EIS was performed on samples over the frequency range 50 kHz-20 mHz. The potential was maintained at the OCP during an experiment with a superimposed perturbation of 20 mV for coated samples and 5 mV for noncoated samples.

Polymer-coated samples.—As previously discussed, due to the lower initial mass of cobalt involved in the Si wafer samples, a lower mass loss increment is possible. During this phase of the work, therefore, Si wafers with a 3200 Å Co layer were employed as the substrate in preference to the Co foils. Figures 7a and b present the EIS data as a function of time for one of the samples (total area of 3.07 cm^2) tested during this phase of the work.

Spectra were assessed by fitting the various components of an equivalent circuit with Zview. This sample revealed two time constants after short immersion and never revealed the primarily capacitive behavior associated with many such coated samples. The phase angle and $|Z|$ curve after 22.5 h reveals two well-defined time constants associated with both the substrate and polymer. After exposure for 59 h both the pore resistance and R_{ct} have increased suggesting the probability that the reduced corrosion is associated with corrosion product deposition within pores. Subsequent to this the pore resistance continued to decrease with time while the corrosion rate increased.

Ultramicrotomy.—One advantage of the transmission electron

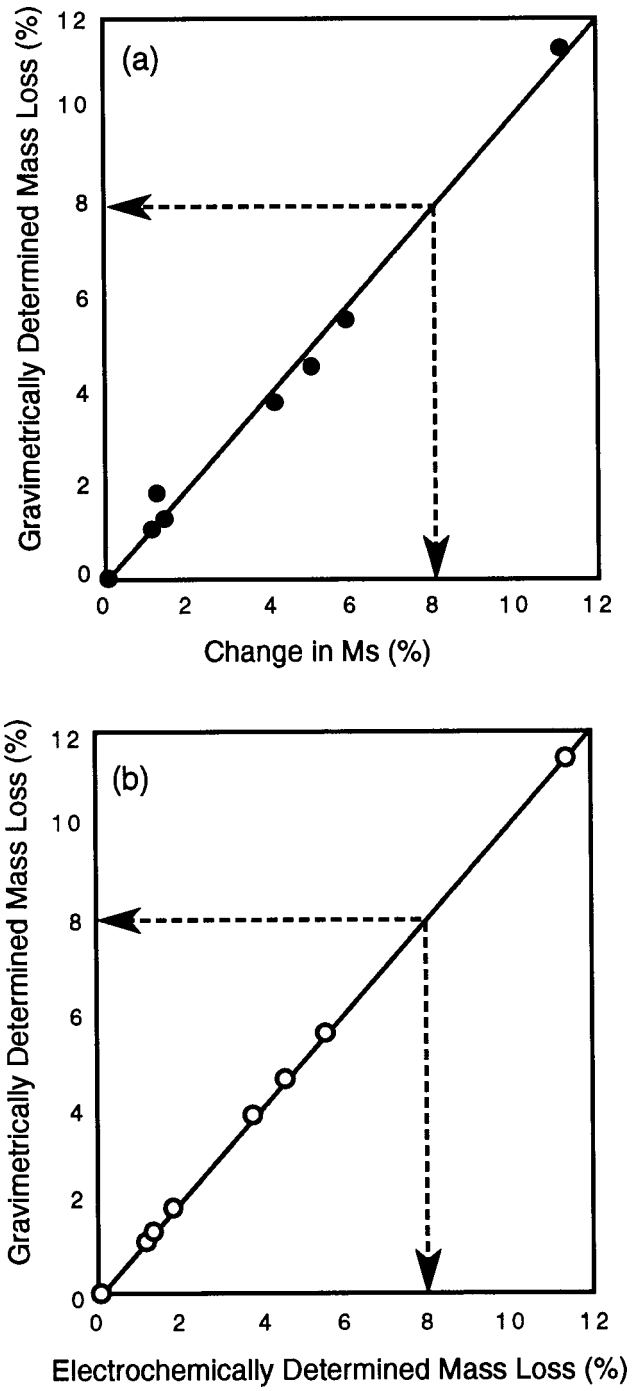

Figure 6. The correlation between the gravimetrically determined mass loss and the mass loss determined (a) magnetically and (b) electrochemically.

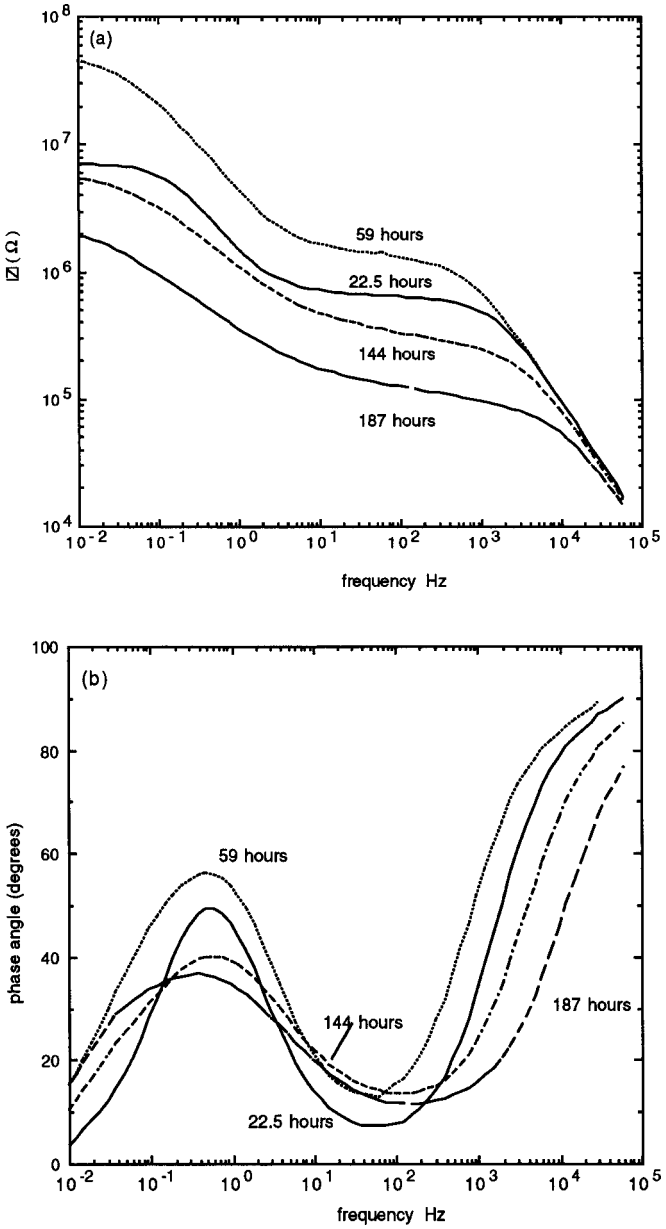

Figure 7. The (a) Bode magnitude and (b) phase angle data as a function of time for one of the samples tested during this phase of the work.

microscope (TEM) is the excellent resolving power and magnification; however, its use requires the production of sections sufficiently thin to allow transmission of electrons. In order to observe samples in cross section during the current research, a TEM was used, in conjunction with thin sections produced at UMIST by ultramicrotomy. To produce an ultramicrotome section, a sample is first embedded in resin and then trimmed with a glass knife to form a truncated pyramid. The extreme end of the specimen block is further trimmed to form a parallel-sided trapezium before presenting the block face to the edge of the diamond knife (see Fig. 8). Ideally, a ribbon of sections is produced and they float on the surface of the liquid (double-distilled water) held in the trough of the diamond knife, located just behind the knife edge. Sections are collected by touching a copper grid to the surface of the liquid, thus, capturing a small droplet of water and sections contained therein. Sections produced in this way are subsequently viewed on the TEM.

Figure 9 presents (a) a surface view of a sample as well as the cross section of (b) the noncorroded and (c) the corroded regions located on the same sample after completion of EIS experiments. The uneven vertical line in the central region of the surface view (Fig. 9a) reveals the demarcation between degraded (right of micrograph) and nondegraded (left of micrograph) regions of the same sample. This demarcation reflects regions of the sample which were either exposed to the electrolyte or shielded from it as a result of cell design. The nondegraded region then reflects the as-received condition of this sample. Not surprisingly, both the dark regions and light colored protuberances within the degraded region revealed elevated chloride levels when analyzed by energy dispersive X-ray (EDX).

In general, it was difficult to obtain ultramicrotome sections for samples used during this research as the Si wafer substrate shattered

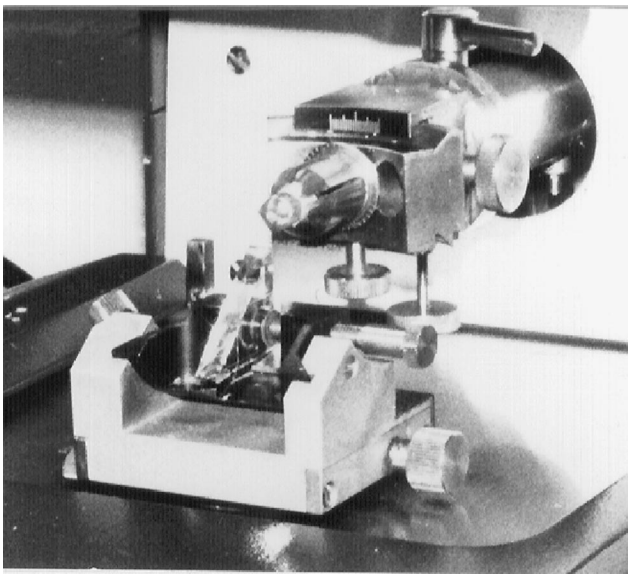

Figure 8. The end of an ultramicrotome sample block face being cut on a diamond knife.

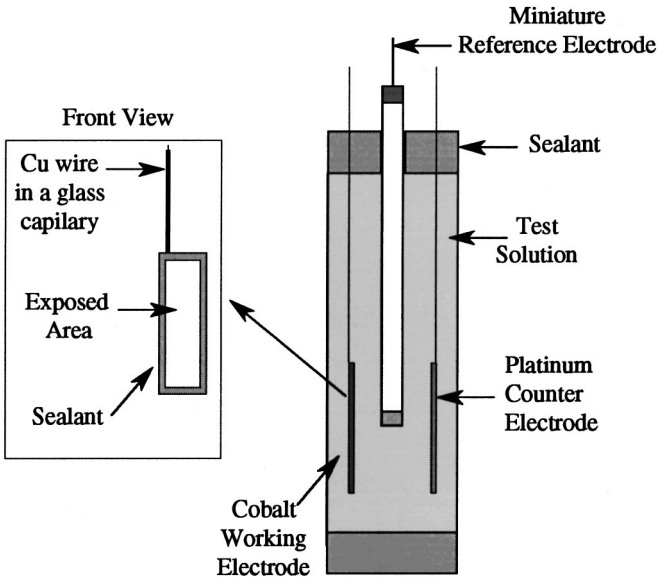

Figure 10. The ultimate cell design employed during the advanced experimental work to permit EIS and VSM *in situ*.

during sectioning with a diamond knife. The sample presented in this figure, however, was successfully detached from the Si wafer, and it was possible in this case to obtain ultramicrotome sections. In both the noncorroded (Fig. 9b) and the corroded regions (Fig. 9c), the dark horizontal band in the center of the TEM micrograph is the cobalt metal layer. Within the noncorroded region (Fig. 9b) this band exhibits a uniform thickness comparable to that of the original Co layer (3200 Å). Conversely, while some areas in the degraded region (Fig. 9c) retain their initial thickness, there are a number of discrete regions that have lost approximately a third of the thickness, indicative of the localized nature of the degradation.

Advanced experimental work.—During this portion of the research,[17] an innovative cell design made it possible to measure mass loss *in situ* and in real time and to correlate VSM and EIS data. The results reveal an excellent correlation between mass loss and EIS for a bare sample; however, interpretation of spectra was more convoluted for the polymer-coated samples.

Cell design.—In order to provide an accurate assessment of the correlation between EIS and mass loss for a coated sample, it was considered important that mass loss be followed *in situ* and in real time. To accomplish this, the constraints of both the electrochemical and magnetic techniques had to be considered during design. This required a sample area large enough for EIS, and small enough to be accommodated within the VSM. In addition, it was imperative that the magnetic character of the cell not interfere with the magnetic measurement and, thus, cell fabrication was intentionally restricted to weakly diamagnetic and paramagnetic materials.

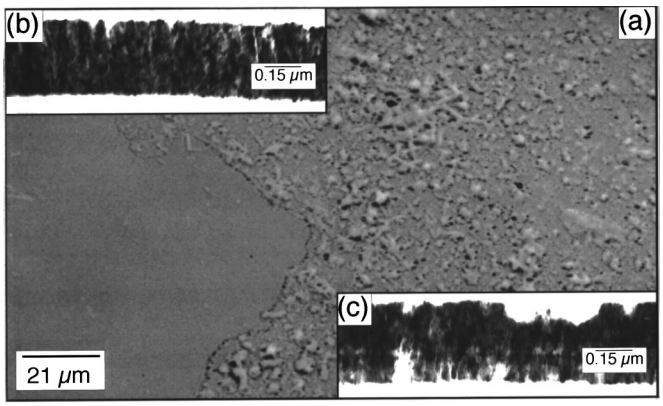

Figure 9. Presents (a) a surface view of a sample as well as the cross section of (b) the noncorroded and (c) the corroded regions located on the same sample after completion of EIS experiments.

The ultimate cell design (Fig. 10) incorporated a three-electrode system. The cell body was formed from a 4.5 cm Pyrex tube having a 1.1 cm inner diameter. One end of the tube was sealed with 5 min epoxy plug and holes for the inner components were subsequently drilled in the hardened plug. A cobalt working (≈0.7 x 2.3 cm) and platinum counter electrode were fixed by epoxy within the cell, and the surfaces of these two electrodes were maintained parallel to each other. The opposite end of the tube and the holes through which the working and counter electrodes were inserted were then sealed with epoxy. A miniature Ag/AgCl reference electrode (EG&G PAR model K0265) was located within the cell during EIS; however, it was removed during magnetic measurement. The hole thus made was sealed with an epoxy plug during VSM measurement. The edges and back of the sample as well as other exposed metal surfaces were masked with Amercoat 90 (Ameron) to obviate contributions from spurious corrosion phenomena. The entire cell assembly was permanently attached with epoxy to a glass rod needed for mounting on the VSM. Prior to initiating experiments, both the individual components and the assembled electrochemical cell were tested on the VSM. Individual components revealed either negligible or low diamagnetic, or paramagnetic behavior. Due to the compensating effect of the opposite slopes of diamagnetic and paramagnetic materials, the ultimate slope of the linear signal from the cell filled with electrolyte was approximately 2.0×10^{-7} emu/Oe. The signal ($\approx 3.5 \times 10^{-2}$ emu) from the cobalt sample was thus predominant making it relatively simple to correct for the slight magnetic character of the cell.

Prior to initiating an impedance measurement, the system was permitted to equilibrate at OCP for a minimum period of 20 min. EIS analysis was carried out for both noncoated and coated samples as a function of exposure time, and in all cases the sample was held potentiostatically at the OCP during data acquisition. The perturba-

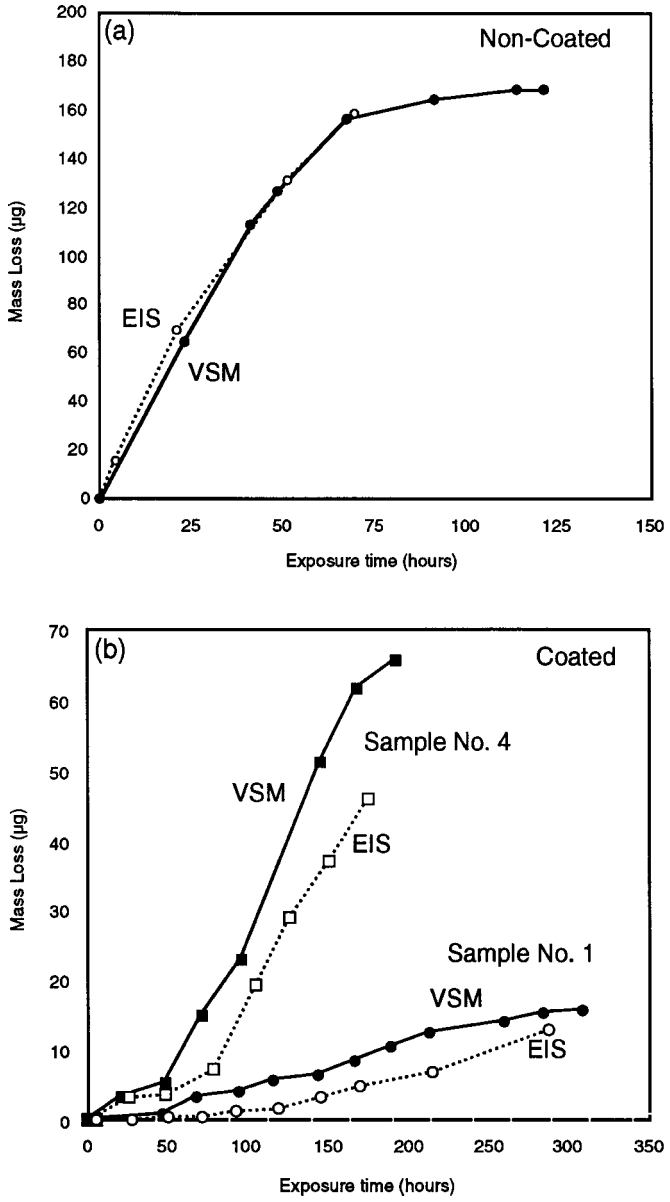

Figure 11. A comparison between the mass loss determined by EIS and VSM for both (a) a noncoated and (b) a coated sample.

tion was 5 and 20 mV for noncoated and coated samples, respectively.

The comparison between the mass loss determined by EIS and VSM for both (a) a noncoated and (b) a coated sample is presented in Fig. 11. For the noncoated sample, the agreement between the data generated by the two measurement techniques to an exposure time of 69 h is excellent. At times longer than 69 h, the plateau in the VSM curve corresponds to the loss of essentially all of the 3200 Å cobalt layer. Subsequent to this, the EIS data became very complex exhibiting multiple time constants. Some portion of this behavior was likely due to the emergence of the Si substrate in regions where the Co layer was totally corroded (see also Fig. 9).

The data presented in Fig. 11b are typical of the results obtained during these experiments for polymer-coated samples. In all cases, a difference was observed in the mass loss data generated by EIS and VSM. Among other potential sources of error, the observed difference may be associated with the extended measurement time required to obtain low frequency EIS data. Alternatively, the Tafel constants employed during analysis were based on values for bare

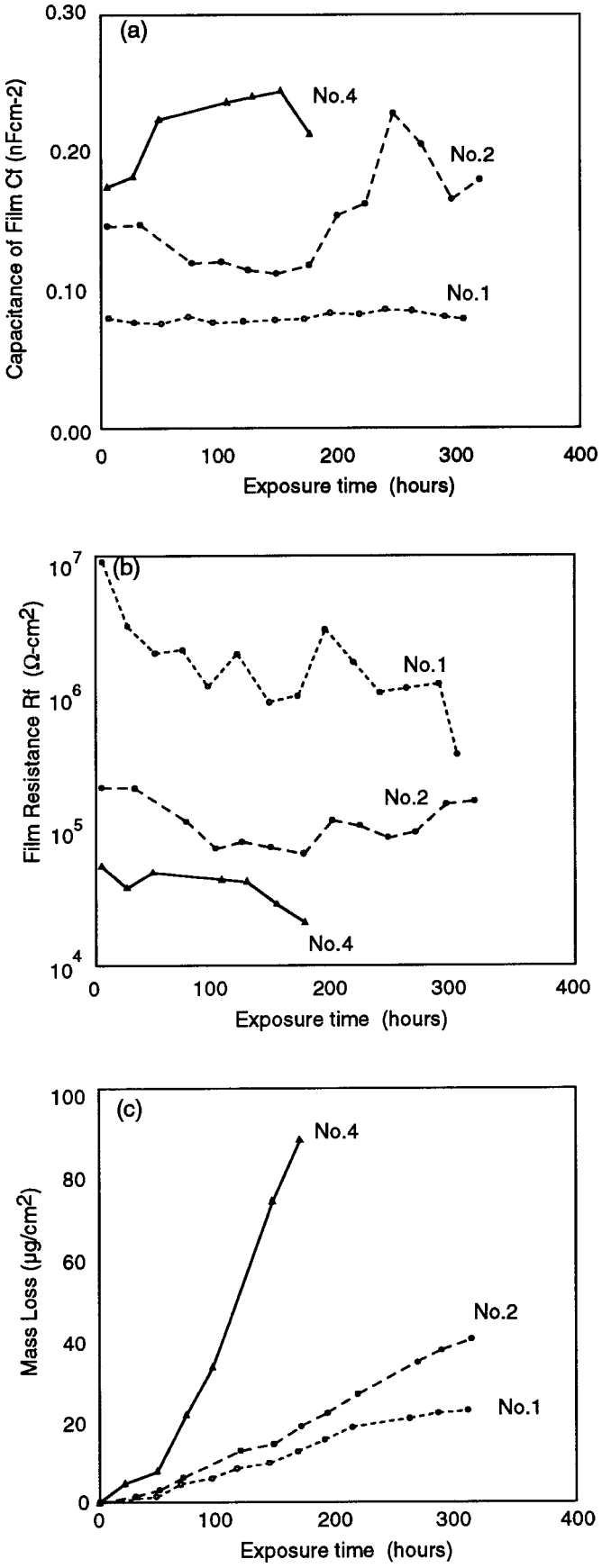

Figure 12. A preliminary real-time analysis of the correlation among (a) coating capacitance, (b) film resistance, and (c) mass loss data for three individual polymer-coated samples.

cobalt in a neutral solution; however, the microenvironment associated with underfilm corrosion will, in general, not be neutral. It is important to note that, qualitatively, EIS was not only able to evaluate the difference between the bare sample and the coated samples but also between the two individual coated samples. The dissimilarity between VSM and EIS mass loss data for the individual coated samples, nevertheless, suggests the need for future research to better define the limitations of the technique in assessing substrate mass loss for polymer-coated metals.

Life prediction of polymer-coated systems.—The ability, in the short term, to predict the longer-term behavior of any system is an attractive concept. Although numerous attempts have been made to correlate various parameters to long-term behavior, there remains considerable uncertainty on the applicability of short-term data to long-term behavior of polymer-coated systems.[18-31]

Figures 12a-c present a preliminary analysis of the correlation among (a) coating capacitance, (b) film resistance, and (c) mass loss data for three individual polymer-coated samples. To our knowledge, these data represent the first accurate real-time correlation between C_f or R_f and substrate mass loss. For the samples assessed during the current project, either R_f or C_f could be employed to rank the degradation of these samples correctly (no. 4 > no. 2 > no. 1). This seemingly corroborates the previous observation that there is a correlation between degradation C_f and R_f for a coated substrate. It is essential, however, to recognize that mass loss could be measured even at very short exposure times and, therefore, corrosion must have initiated almost immediately after immersion in the electrolyte. The current data, therefore, provide no indication of the applicability of these parameters for more protective coatings.

While the data presented in this section do provide some insight into the potential capability of EIS to provide predictive information on the corrosion character of a polymer-coated metal, clearly further research is needed to evaluate the applicability of this technique for various coated systems, and this will be the subject of a future study.

Conclusions

This paper addresses some unresolved issues remaining in spite of significant research in the area of protective organic coatings. During this study, the metallic mass loss for a polymer-coated metal has been assessed *in situ* and in real time and correlated to data produced by EIS. This has been accomplished by a unique combination of magnetic (VSM) and electrochemical (EIS) techniques. The relationship between EIS data and loss of substrate metal for a polymer-coated sample has unequivocally been established for the samples investigated during this project.

During the preliminary experimental work, mass loss assessed by gravimetric, electrochemical, and magnetic methods was compared, and the data indicated a 1:1 relationship. Ultramicrotomy was used in combination with TEM to reveal the sample cross section, and the localized nature of the degradation.

During the advanced phase of the research, an innovative cell design made it possible to correlate VSM and EIS data *in situ* and in real time. For noncoated samples, the agreement between EIS and VSM data was excellent. While there was an appreciable difference in the mass loss assessed by VSM and EIS for the coated samples, qualitatively, EIS was not only able to evaluate the difference between the bare sample and the coated samples but also between individual coated samples.

The coating parameters C_f and R_f were both capable of ranking the coated samples correctly however, research is still needed to assess the applicability of these parameters for systems incorporating more protective coatings.

Acknowledgments

This material is based upon work supported by the National Science Foundation under grant no. 9708148.

Massachusetts Institute of Technology assisted in meeting the publication costs of this article.

References

1. W. J. Lorenz and F. Mansfeld, *Corros. Sci.*, **21**, 647 (1981).
2. F. Mansfeld and M. Kendig, Rockwell International Science Center Report no. SC5222.FR (1986).
3. M. Stern and A. Geary, *J. Electrochem. Soc.*, **104**, 59 (1957).
4. F. Mansfeld, *J. Appl. Electrochem.*, **25**, 187 (1995).
5. G. Walter, *Corros. Sci.*, **26**, 681 (1986).
6. B. Hepburn, L. Callow, and J. Scantlebury, J. Oil Colour Chem. Assoc., **1984**, 193.
7. B. Hepburn, K. Gowers, and J. Scantlebury, *Br. Corros. J., London*, **21**, 105 (1986).
8. F. Mansfeld, *Corrosion (Houston)*, **36**, 301 (1981).
9. J. R. Macdonald, *Impedance Spectroscopy*, p. 306, John Wiley & Sons, New York (1987).
10. D. B. Mitton, Ph.D. Thesis, University of Manchester Institute of Science and Technology, Manchester, U. K. (1989).
11. S. L. Wallace M.S. Thesis, Massachusetts Institute of Technology, Cambridge, MA (1999).
12. S. Foner, *Rev. Sci. Instrum.*, **30**, 548 (1959).
13. A. Zieba and S. Foner, *Rev. Sci. Instrum.*, **53**, 1344 (1982).
14. C. Johanson and M. Hanson, *IEEE Trans. Magn.*, **30**, 1064 (1994).
15. W. Betteridge, *Cobalt and Its Alloys*, Ellis Horwood Limited, England (1982).
16. R. Bozoroth, *Ferromagnetism*, p. 293, IEEE Press, New York (1951).
17. N. J. Cantini, M.S. Thesis, Massachusetts Institute of Technology, Cambridge, MA (2000).
18. R. E. Touhsaent and H. Leidheiser, *Corrosion (Houston)*, **28**, 435 (1972).
19. J. R. Scully, *J. Electrochem. Soc.*, **136**, 979 (1989).
20. F. Deflorian, L. Fedrizzi, S. Rossi, F. Buratti, and P. L. Bonora, *Prog. Org. Coat.*, **39**, 9 (2000).
21. H. S. Isaacs, A. J. Davenport, J. Hawkins, and G. E. Thompson, *Corros. Sci.*, **33**, 1141 (1992).
22. J. Titz, G. H. Wagner, H. Spähn, M. Ebert, K. Jüttner, and W. J. Lorenz, *Corrosion (Houston)*, **46**, 221 (1990).
23. I. Sekine, *Prog. Org. Coat.*, **31**, 73 (1997).
24. G. Walter, *Corros. Sci.*, **26**, 681 (1986).
25. F. Mansfeld, *Corrosion (Houston)*, **44**, 856 (1988).
26. M. Kendig, F. Mansfeld, and S. Tsai, *Corros. Sci.*, **24**, 317 (1983).
27. R. Bacon, J. Smith, and F. Rugg, *Ind. Eng. Chem.*, **40**, 161 (1948).
28. M. Kendig and J. Scully, *Corrosion (Houston)*, **46**, 22 (1990).
29. P. Bonora, F. Deflorian, and L. Fedrizzi, *Electrochim. Acta*, **41**, 1074 (1996).
30. F. Mansfeld, *J. Appl. Electrochem.*, **25**, 187 (1995).
31. J. N. Murray, *Prog. Org. Coat.*, **31**, 375 (1997).